Predicting Oxide Stability in High-Temperature Water Vapor

Elizabeth J. Opila, Nathan S. Jacobson, Dwight L. Myers, and Evan H. Copland

The importance of understanding and predicting the interactions of oxides with water vapor at high temperatures is demonstrated in this article. Methods for observing volatilization phenomena and identifying the chemical formulae for volatile metal hydroxides are discussed. In addition, techniques for obtaining accurate thermodynamic data for gaseous metal hydroxide species are described. Detailed examples of the stability of the principle structural and/or protective oxides chromia (Cr_2O_3), silica (SiO_2), and alumina (Al_2O_3) in high-temperature water vapor are included.

INTRODUCTION

Many oxide phases, either as structural ceramics or thermally grown scales on alloys or non-oxide ceramics, find application in high-temperature corrosive environments because of their thermodynamic stability. Applications with severe environments include heat engines, heat exchangers, power and propulsion technologies, material fabrication processes, and waste incineration. Many of these environments contain substantial amounts of high-temperature water vapor, found as a component of the ambient atmosphere or as a product of combustion. The interaction of high-temperature water vapor with oxides to form volatile hydroxides leads to material loss which can be a life-limiting degradation mechanism. A generic reaction that describes oxide material loss by formation of volatile hydroxides is shown in Equation 1, where M denotes a metal atom or ion. (Note: All equations are given in the table on page 24.) The formation of volatile hydroxides depends in some cases on both the water vapor and oxygen partial pressures in the process environment. It has been shown that when the equilibrium vapor pressure of a volatile species is 10^{-7} MPa or greater, material loss due to volatility becomes an important consideration for long-term applications.[1,2] Table I shows upper temperature limits, based on this 10^{-7} MPa criterion, for several oxides in various gas environments to illustrate how significantly water vapor can limit application temperatures. In order to make these chemical lifetime predictions for materials in high-temperature water vapor environments, the overall degradation mechanism must be understood and accurate thermodynamic data must be available for the key reactions.

Table I. Approximate Upper Use Temperature (°C) for Oxides Based on Partial Pressure of all Volatile Species Equal to 1×10^{-7} MPa

	Air: 0.1 MPa Total 2.1×10^{-2} MPa O_2 10^{-3} MPa H_2O	0.1 MPa Total 10^{-2} MPa O_2 10^{-2} MPa H_2O	1 MPa Total 0.1 MPa O_2 0.1 MPa H_2O
Cr_2O_3	1,122	1,042	499
SiO_2	1,575	1,370	967
Al_2O_3	M	1,864	1,345

M= material limited by melting point of oxide rather than volatility.

See the sidebar for experimental procedures.

IDENTIFICATION OF VOLATILE SPECIES

Once a volatilization phenomenon has been observed, it is important to identify the volatile vapor species so that volatility rates can be predicted. The identity of the volatile species can be determined in several ways. The most obvious method of identifying vapor species is by determining the stoichiometry of Equation 1. The volatility rate will depend on $P(H_2O)^n$ and $P(O_2)^m$. The quantification of the power law exponents n and m allow the chemical formula of the volatile species to be determined. The power law exponents can be determined by measuring the volatility rate using the previously described techniques (weight loss, recession, or downstream transport) as the water vapor and oxygen partial pressure are varied systematically with all other experimental conditions held constant.

High-temperature mass spectrometry

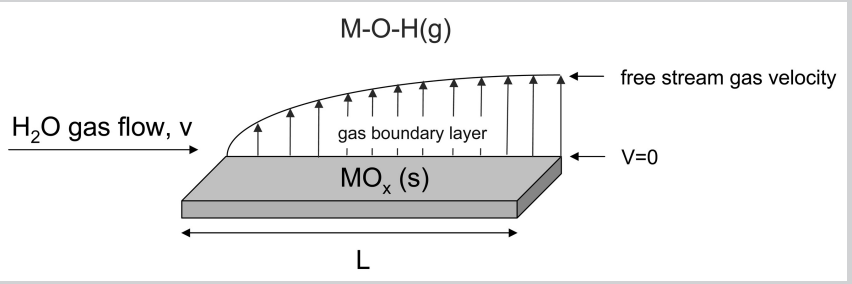

Figure 1. A schematic drawing of metal oxide (MO_x) volatility to form a gaseous hydroxide (M-O-H(g)). The volatilization rate is limited by M-O-H(g) transport outward through a laminar gas boundary layer at free stream gas velocity, v. L is the characteristic length dimension as shown in Equation 2.

has been used with tremendous success to identify many high-temperature species. In general, species identification is made using the Knudsen effusion mass spectrometry technique.[11] The material of interest is enclosed in a Knudsen cell which is placed in the low-pressure reducing environment of the vacuum mass spectrometer. The vapor species diffuse through a small orifice, and then are ionized and accelerated into the mass spectrometer for identification by mass-to-charge ratio. In some cases, gas leak Knudsen effusion studies have been conducted where low pressures of water vapor were introduced into the Knudsen cell so that hydroxide vapor species could be identified.[12–14] However, these studies are limited to reactant water vapor pressures of about 10^{-6} MPa or less.

The applications discussed in this paper generally involve much higher oxygen and water vapor partial pressures than those that can be tolerated in a Knudsen effusion mass spectrometer. A unique type of mass spectrometer has proven valuable in identifying hydroxides at these higher pressures.[15,16] Free jet sampling mass spectrometry allows sampling of a 0.1 MPa gas stream, expansion of the gas stream to quench in the vapor species, and finally mass filtering at the low pressures needed to identify vapor molecules by mass-to-charge ratio. Mass spectrometry is very useful, but requires sophisticated equipment, and the identification of the vapor species can be complicated by fragmentation of the vapor molecules during the ionization process. Ideally, the combination of mass spectrometry and pressure-dependent volatility studies should be conducted for unequivocal species identification.

DETERMINATION OF ACCURATE THERMODYNAMIC DATA

As noted, accurate thermodynamic data are critical for effective modeling and prediction of chemical lifetimes. There are many methods for obtaining such data for inorganic vapors.[17] The transpiration method is most useful for identifying volatile hydroxides. The transpiration technique is a well-established and versatile technique for studying gas-solid equilibria and measuring vapor pressures in the presence of large concentrations of other gases.[18] The reactive gases, oxygen and water vapor, and in some cases a nonreactive carrier gas such as argon, flow over oxide pellets which are contained in a reaction cell. Flow rates are chosen to eliminate any diffusion effects or kinetic limitations so that the equilibrium pressure of volatile hydroxide species can be established in the reaction chamber. Volatile M-O-H species flow into cooler condensation

EXPERIMENTAL PROCEDURES

Typically, the volatile hydroxides formed from chromia, silica, and alumina have vapor pressures near 10^{-7} MPa, depending on temperature and water vapor pressure conditions. However, volatility may go unnoticed in short-term laboratory exposures unless extra care is taken in interpreting experimental results.

High-temperature water vapor for laboratory experiments is typically generated in two ways. First, a gas stream can be saturated with a controlled amount of water vapor by bubbling a carrier gas through a temperature-controlled water bath.[3] An alternative technique is to directly inject a controlled amount of liquid water into a hot carrier gas stream flowing at a known rate.[4] The water vapor/carrier gas mixture then flows over a sample coupon of the material to be studied. Since volatility rates depend on the linear gas velocity, it is critical that the total linear gas velocity over the sample at the test temperature be reported for volatilization experiments. This information is needed so that experiments can be duplicated and volatilization kinetics can be modeled.

The most obvious way to detect volatility of a material is by measuring weight loss, either continuously by thermogravimetric analysis or by interrupted weight-change measurements. This technique is simple and straightforward and has been used for bulk oxides.[5–7] If, however, a nonoxide material is exposed in high-temperature water vapor, the water vapor can act as an oxidant resulting in growth of an oxide scale with a corresponding mass gain. If the oxide simultaneously forms a volatile hydroxide, the mass loss due to volatility can be masked by the oxidation weight gain. The weight change kinetics in this case follow a paralinear rate law.[8,9] Initially a mass gain is observed, followed by mass loss, as shown in Figure A. Eventually a steady-state mass loss rate is achieved that may only be observable after tens or hundreds of hours, depending on the relative rates of oxidation and volatilization.[10]

Alternatively, volatility of a material can be identified by observed consumption or recession of a material. Material recession can be difficult to measure for short-term laboratory exposures when, for example, several micrometers of material are lost from a sample coupon of millimeter-scale dimensions. For nonoxide materials exposed in high-temperature water vapor, the thickness of a thermally grown oxide scale can generally be easily measured after exposure by observation of the coupon cross section with optical or electron-optical microscopy. In the case of thermal oxidation without volatility, the weight gain due to oxidation can be predicted from the measured oxide thickness if the density of the oxide is known. The measured weight gain should be in good agreement with the weight gain predicted from the oxide scale thickness. If both oxidation and volatilization of a nonoxide material occurs, the weight gain calculated from the oxide thickness will be larger than the measured weight change. This discrepancy between measured and calculated weight change is an indirect way to confirm oxide volatility for nonoxide materials.[9]

Finally, simple observations can be made to identify volatilization processes. Surface rearrangement of oxide surfaces leaving well-defined surface faceting or etching is indicative of a vapor phase process.[5] Other methods are needed to confirm that this is a volatilization process rather than surface diffusion or thermal etching. Similarly, deposits of the material of interest found in cooler locations downstream of the exposed sample are definite signs of volatility. Under carefully controlled conditions, the volatility rate can be quantified by measuring the amount of material transported downstream.

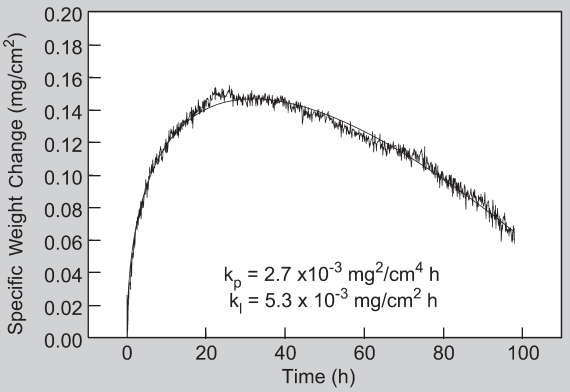

Figure A. The paralinear weight change of CVD SiC exposed at 1,200°C, 5x10^{-2} MPa H_2O(g), 5x10^{-2} MPa O_2(g), and 4.4 cm/s gas velocity. The parabolic oxidation rate constant, k_p, and the linear volatilization rate constant, k_l, are shown.

Table II. Parameters Used in Equation 2

Symbol	Definition	Units	Comments
Δw	Weight change	mg	Measured from experiment or predicted if P is known or calculated
A	Surface area of coupon	cm^2	Measured
t	Exposure time	h	Experimental variable
ρ'	Density of gas boundary layer	g/cm^3	Calculated from ideal gas law
v	Gas velocity	cm/s	Experimental variable
L	Characteristic length	cm	Length of coupon
η	Gas viscosity of boundary layer	g/(cm/s)	Obtained from tabulated values
D	Interdiffusion coefficient of volatile species in laminar boundary layer	cm^2/s	Calculated from Chapman Enskog Equation. See Reference 21
P	Partial pressure of volatile species	MPa	Unknown quantity to be calculated or predicted from thermodynamic data
M	Molecular weight of volatile species	g/mol	
R	Gas constant	$(cm^3$ atm)/K mol	
T	Absolute temperature	K	Experimental variable

tubes and condense along with the water vapor. The deposits, and if necessary, the condensed water are collected and quantitatively analyzed for the amount of metal atoms, M. Knowing the moles of oxygen and water vapor input as well as the moles of M collected, the equilibrium constant for the volatility reaction can be determined. The enthalpy and entropy of reaction can be determined from the temperature dependence of the equilibrium constant. These types of studies have been conducted for the SiO_2-H_2O-O_2 system,[19,20] for example. Alternatively, for materials with high enough volatility, the weight loss of the material in the transpiration cell can be determined if chemical analyses cannot be conducted. This technique has been used to study chromia volatility in high-temperature water vapor.[6] Both transpiration techniques, condensate collection and sample weight loss, rely on the attainment of chemical equilibrium in the reaction cell.

Weight loss techniques can also be used for flat plate sample coupons in well-defined laminar flow conditions. In this case, the measured mass flux, J, together with the semi-empirical kinetic expression for laminar flow over a flat plate can be used to determine the equilibrium partial pressure of the volatile species. This semi-empirical relationship has been described in detail[21,22] and is given by Equation 2. The term in the first parentheses is the dimensionless Reynolds number, while the term in the second set of parentheses is the dimensionless Schmidt number. The symbols are defined in Table II. This expression is applicable when volatility is limited by transport of the volatile species outward through a laminar gas boundary layer, as illustrated in Figure 1. This technique has been used to determine the partial pressure of $Al(OH)_3(g)$ as a function of temperature and water vapor partial pressure in the Al_2O_3-H_2O-O_2 system.[5]

Finally, computational techniques can be used to calculate thermodynamic properties for gas species. This is the only practical method for generating thermodynamic properties across systems in which a large range of molecules are possible and in cases where experiments are not easily interpreted due to the presence of more than one volatile species. In the past, molecular geometries and properties of similar molecules were used quite successfully to estimate thermodynamic properties of gas molecules using standard formulations from statistical mechanics.[23] More recently, ab-initio computational methods[24] have been used to calculate the molecular geometry and vibrational frequencies. These, together with a first-principle calculation of the heat of formation, are used to generate thermochemical properties for the molecule of interest.

Given known thermodynamic data for a volatilization reaction and a valid kinetic expression such as Equation 2, the flux of that species, and thus the recession rate of the oxide, can be predicted over the range of conditions of interest.

OXIDE STABILITY IN HIGH-TEMPERATURE WATER VAPOR: EXAMPLE SYSTEMS

$Cr_2O_3 + H_2O(g)$

Chromia-forming materials are used in a variety of applications that contain high-temperature water vapor. The application environments result in chromia volatilization reactions. These applications include fuel cell interconnects[25,26] and structural steels[27,28] for heat exchang-

Equations

$$MO_x + nH_2O(g) + mO_2(g) = MO_{(x+n+2m)}H_{(2n)}(g) \quad (1)$$

$$J = \frac{\Delta w}{At} = 0.664\left(\frac{\rho' vL}{\eta}\right)^{1/2}\left(\frac{\eta}{\rho' D}\right)^{1/3}\frac{DPM}{LRT} \quad (2)$$

$$\tfrac{1}{2}\,Cr_2O_3(s) + \tfrac{3}{4}\,O_2(g) = CrO_3(g) \quad (3)$$

$$\tfrac{1}{2}\,Cr_2O_3(s) + H_2O(g) + \tfrac{3}{4}\,O_2(g) = CrO_2(OH)_2(g) \quad (4)$$

$$\tfrac{1}{2}\,Cr_2O_3(s) + \tfrac{1}{2}\,H_2O(g) + \tfrac{1}{2}\,O_2(g) = CrO_2(OH)(g) \quad (5)$$

$$\frac{dx}{dt} = \frac{k_p}{2x} - k_l \quad (6)$$

$$SiO_2(s) + 2H_2O(g) = Si(OH)_4(g) \quad (7)$$

$$SiO_2(s) + H_2O(g) = SiO(OH)_2(g) \quad (8)$$

$$SiO_2(s) + \tfrac{1}{2}\,H_2O(g) = SiO(OH)(g) + \tfrac{1}{4}\,O_2(g) \quad (9)$$

$$SiO_2 = SiO(g) + \tfrac{1}{2}\,O_2(g) \quad (10)$$

$$\tfrac{1}{2}\,Al_2O_3(s) + 3/2\,O_2(g) = Al(OH)_3(g) \quad (11)$$

ers or recuperators. Chromia volatility is also a problem in waste incineration,[29] steam-methane reforming,[30] and chemical vapor deposition reactors.[31]

It is well known that chromia volatilizes in oxidizing environments by the reaction shown in Equation 3.[6–8,32] Volatility is enhanced in water vapor by the reactions shown in Equation 4 and Equation 5.[6,7,29,33–36] Note that the formation of these oxyhydroxide species depends on both the water vapor and the oxygen partial pressures. While the Cr_2O_3-H_2O-O_2 system has been studied extensively, the identity of the predominant volatile oxyhydroxide species was still uncertain and there was little agreement on the thermodynamic stability of these species.[29,34,37,38] A recent study clarifies some of these issues.[39] Transpiration experiments were conducted at 600°C as a function of both water vapor and oxygen partial pressure at 0.1 MPa total pressure. The results, shown in Figure 2, confirm that the volatility shows power law dependences of 1 and ¾ for water vapor and oxygen, respectively, consistent with Equation 4. This reaction is expected to dominate up to temperatures of at least 900°C. At temperatures of 1,300°C and higher, Kim and Belton[6] demonstrated that Reaction 5 dominates, although Reaction 3 is also important at these temperatures. The temperature dependence of Reaction 4 was also determined recently between 300°C and 900°C using the transpiration method[39] and is shown in Figure 3 compared to other data available from the literature. The data from this study[39] are recommended.

The Cr_2O_3-H_2O-O_2 system is very complex and many volatile species, in addition to the three previously discussed, are possible. Ebbinghaus[29] has compiled a thorough review and assessment of the data available before 1992. Using Ebbinghaus' data the authors have calculated the equilibrium partial pressure of volatile Cr-O-H species from the reaction of chromia with 10^{-2} MPa water vapor partial pressure and 10^{-2} MPa oxygen partial pressure to show the complexity of the system as shown in Figure 4. Espelid et al.[38] have made ab-initio calculations for a variety of Cr-O-H species. There is a considerable degree of uncertainty in these results, due to the large number of possible electronic states available to chromium, as is true for all transition metal compounds. Nevertheless, thermochemical data in this system are often in disagreement or missing, so these ab initio calculations are a valuable contribution.

Chromia-forming alloys undergo simultaneous oxidation and volatilization reactions in oxidizing environments. Tedmon[8] has modeled the kinetics of these reactions for chromium and Fe-Cr alloys in the case of $CrO_3(g)$ formation with a paralinear model. This model can be expressed in its simplest form (see Equation 6) where x is oxide thickness, t is time, k_p is the parabolic oxidation rate constant ($\mu m^2/h$), and k_l is the linear volatilization rate constant ($\mu m/h$). Alternatively, this equation can be expressed in terms of material recession or weight change. These expressions can be integrated and solved numerically.[9] Paralinear kinetics will also be observed for the exposure of chromia-forming alloys in water vapor with $CrO_2(OH)_2(g)$ formation.

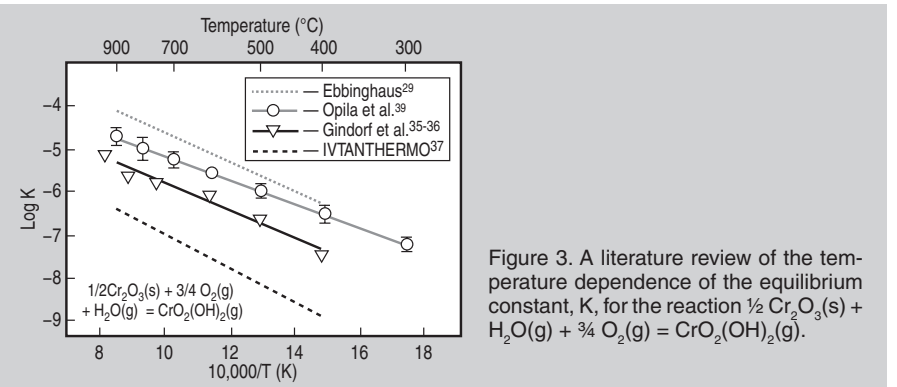

Figure 3. A literature review of the temperature dependence of the equilibrium constant, K, for the reaction ½ $Cr_2O_3(s)$ + $H_2O(g)$ + ¾ $O_2(g)$ = $CrO_2(OH)_2(g)$.

SiO_2-H_2O

Silica-forming materials are also used in a variety of applications that contain high-temperature water vapor resulting in silica volatilization. Materials of interest include structural ceramics (SiC composites and Si_3N_4)[40–43] and alloys ($MoSi_2$ and other refractory silicides)[44,45] for power and propulsion applications. Silica volatilization by hydroxide formation is also a concern in geological[46] and cosmological processes.[19] Finally, silicon hydroxide vapor species are important in chemical vapor deposition processes.[47]

The SiO_2-H_2O system has been well studied in the past decade. It has been confirmed that for processes at 0.1 MPa and temperatures below about 1,300°C silica volatility can be attributed to the reaction shown in Equation 7. This has been determined through mass spectrometry studies[48] as shown in Figure 5, as well as pressure-dependent transpiration[19,20] and weight-loss measurements.[42,49] Thermodynamic data have been determined for $Si(OH)_4(g)$ using the transpiration method[19,20] as well as ab initio calculations.[47] These data are in agreement, as shown in Figure 6.

At higher temperatures and lower water vapor and oxygen partial pressures Reactions 8 and 9 can become more important,[12,13,20] with SiO(OH)(g) more stable under reducing conditions.

Thermodynamic data have been acquired for $SiO(OH)_2(g)$ by mass spectrometry[12,13] and transpiration.[20]

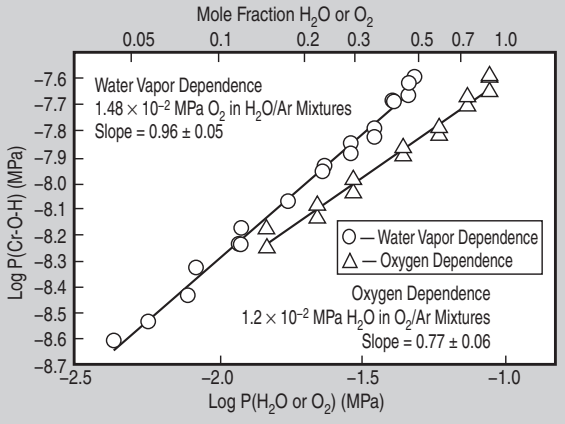

Figure 2. The determination of the volatile Cr-O-H species identity formed from $Cr_2O_3(s)$ + $H_2O(g)$ + $O_2(g)$ at 600°C using the transpiration technique. The volatility depends on $P(H_2O)^{0.96}$ and $P(O_2)^{0.77}$ consistent with $CrO_2(OH)_2(g)$ formation by Equation 4.

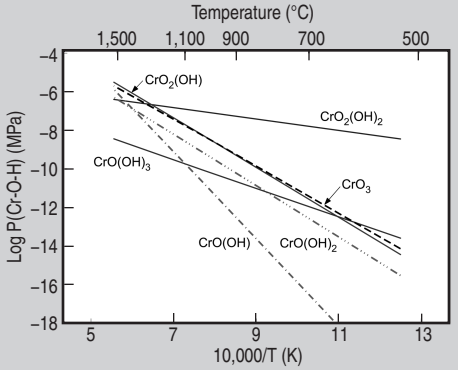

Figure 4. The temperature dependence for volatile Cr-O-H(g) species calculated at 10^{-2} MPa H_2O(g) and 10^{-2} MPa O_2(g) using the thermodynamic data of Ebbinghaus.[29]

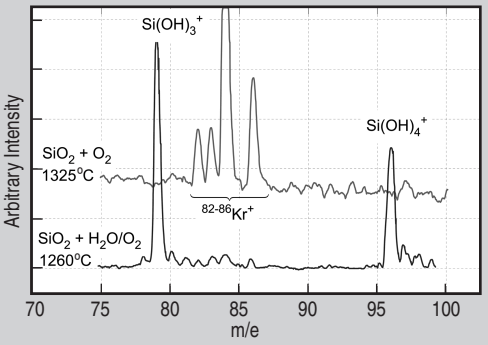

Figure 5. The mass spectra of SiO_2 + O_2(g) and SiO_2 + H_2O(g) + O_2(g) obtained using free jet sampling mass spectrometry. The krypton found in the oxygen acts as a standard for mass-to-charge ratio, m/e. $Si(OH)_4$(g) is found in the H_2O(g) containing exposure: the $Si(OH)_3^+$ fragment ion at m/e=79 and the $Si(OH)_4^+$ parent ion at m/e=96.

Thermodynamic data for SiO(OH)(g) have also been determined by mass spectrometry.[12,13] Experimental data for SiO(OH)(g) and $SiO(OH)_2$(g) are less certain due to both scarcity of results and the difficulty in obtaining them. Thermodynamic data from ab-initio calculations are also available for both these oxyhydroxide species.[47,50]

At high temperatures and conditions with low-oxygen partial pressures, SiO(g) formed by Reaction 10 can be found in significant quantities even in the presence of water vapor. Thermodynamic data for SiO(g) are available in standard thermodynamic data bases such as the JANAF tables.[51]

Silica-forming materials, rather than bulk silica, are typically used in applications of technological interest. Thus oxidation and volatilization of these non-oxide materials in the presence of water vapor are of interest. Silicon and thermally grown silica passivation layers are widely used in the microelectronics industry. While oxidation of silicon is sometimes conducted in water vapor[52] or hydrogen/oxygen mixtures to form water vapor, volatility of silica is not observed under normal processing pressures, gas flow rates, and times. SiC composites and Si_3N_4 are under development for structural components of gas turbines for power and propulsion applications. Water vapor, present as a product of combustion, is present at high pressure, temperature, and gas velocity. In addition, the desired lifetimes of combustor liners and turbine vanes and blades are on the order of 10,000 h. Under these conditions, volatility of the thermally grown silica scales is a life-limiting issue.[42,43,49] Paralinear kinetics as described by Equation 6 are observed in these combustion conditions.[40,49] Because the exposure lifetimes are so long, however, the kinetics can be approximated by the linear volatility rate of silica and corresponding recession rate of the underlying material alone.[10] Under high-velocity conditions, laminar flow will give way to turbulent flow. For turbulent flow conditions, the volatility rate given by Equation 2 requires modification. The primary difference is that the Reynolds number and thus the gas velocity dependence increase from 0.5 for laminar flow to 0.8 for turbulent flow.[22] While the paralinear oxidation/volatilization kinetics are well characterized for SiC and Si_3N_4, the kinetic models will hold true for other silica formers such as molybdenum silicides and niobium silicides.

Despite the silica volatility issues just described, SiC and Si_3N_4 materials are still attractive because of the high-temperature mechanical properties they offer compared to the current superalloys. As a result, environmental barrier coatings (EBCs) have been developed for silica-forming ceramics to limit volatility.[53–55] Because good chemical compatibility as well as good thermal expansion match to these ceramics are needed, many of the proposed EBCs are silicates, such as barium strontium aluminosilicates (BSAS)[56] and rare earth (RE) silicates of the $RESi_2O_5$ structure.[57] Silica will still volatilize from these materials but at a reduced rate due to the lower silica activity in these compounds. A necessary requirement for EBCs is thus a low-silica activity as well as a low activity of any other volatile oxides. Barium strontium aluminosilicates and $RESi_2O_5$ function well as EBCs because of their lower-than-ideal silica activities.

Al_2O_3-H_2O

Alumina and alumina-forming materials are used in a variety of applications that contain high-temperature water vapor. Superalloys rely on the formation of protective alumina scales for use in turbine engines for power and propulsion applications. Alumina is also being considered for use in combustion environments as a component of oxide/oxide composites[58] or as a constituent of high-temperature coatings.[59]

Alumina is known to volatilize in high-temperature water-vapor-containing environments by Equation 11. This has been demonstrated by the pressure-dependent transpiration experiments for calcium aluminate[19] and sapphire coupon weight loss experiments.[5] Surface rearrangement of ground sapphire coupon edges after exposure in high-temperature

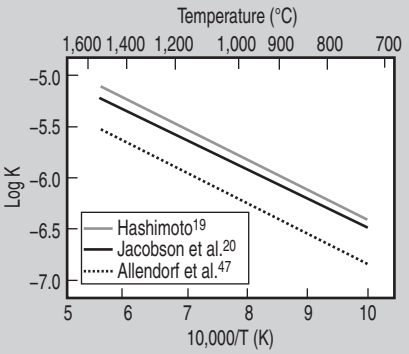

Figure 6. A literature review of the temperature dependence of the equilibrium constant, K, for the reaction SiO_2(s) + $2H_2O$(g) = $Si(OH)_4$(g).

water vapor was very striking in this material system as shown in Figure 7.

Thermodynamic data for $Al(OH)_3(g)$ are available from several sources. IVTANTHERMO[37] includes data derived by estimation from similar molecules such as $AlF_3(g)$. Hashimoto experimentally determined thermodynamic data for $Al(OH)_3(g)$ as already described.[19] Finally, ab initio results for this species are also available.[60] The data from all sources are in excellent agreement, as shown in Figure 8.

Volatility of alumina is not an issue for superalloys currently used in turbine engines because the use temperatures are too low, at 1,200°C and lower. Alumina volatility by $Al(OH)_3(g)$ formation is not expected to be a problem below about 1,300°C even for long-term applications. However, if alumina-based composites and coatings are used at higher temperatures, $Al(OH)_3(g)$ formation could be life-limiting for these materials.

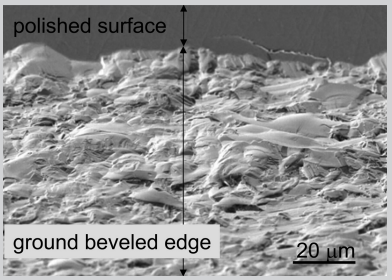

a

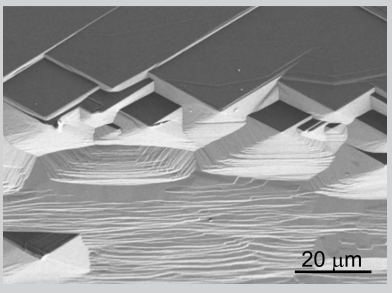

b

Figure 7. Scanning electron micrographs of sapphire coupon edges demonstrating surface rearrangement observed after water vapor exposures. (a) As-received coupon. (b) Coupon after treatment for 72 h at 1,450°C in 6.9 x 10^{-2} MPa H_2O/3.2 x 10^{-2} MPa O_2 flowing at 4.4 cm/s.

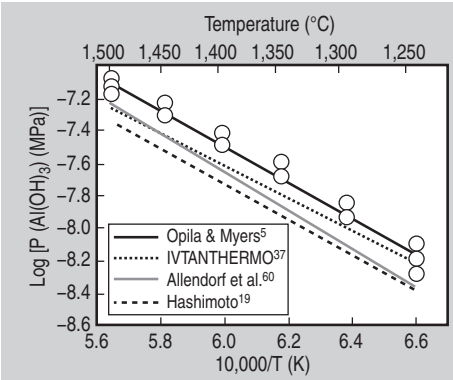

Figure 8. A literature review of the temperature dependence of the $Al(OH)_3(g)$ partial pressure for the reaction 1/2 $Al_2O_3(s)$ + 3/2 $H_2O(g)$ = $Al(OH)_3(g)$.

Additional Technologically Important Oxides—H_2O Systems

Two additional oxides that show very low and very high stability in high-temperature water vapor are boria (B_2O_3) and zirconia (ZrO_2). Both of these oxides are of technological interest. Boria is present as an oxidation product from B_4C and BN phases often used in ceramic matrix composites as oxidation inhibitors or as interphases between fibers and matrices.[61,62] Boria is a product of oxidation of ZrB_2 and HfB_2. These compounds are the basis for ultra-high-temperature ceramics (UHTCs) which are receiving new interest for hypersonic vehicle leading edges or missile propulsion systems.[63] Finally, boria is also an oxidation product in alloy systems such as Mo-Si-B and Nb-Si-B, which are currently under development for high-temperature turbine applications.[64,65] Despite the wide applicability of boria-forming materials, boria is very unstable in water vapor. Several volatile B-O-H species are stable including BO(OH), $[BO(OH)]_3$, and $B(OH)_3$.[14] Volatile boron hydroxides are known to form in significant amounts at relatively low temperatures when even ppm-levels of water vapor are present in the environment.[66]

Yttria-stabilized zirconia (YSZ) is the standard thermal barrier coating used for superalloys in turbine applications. YSZ is very stable in water-vapor-containing combustion environments at current application temperatures up to 1,200°C. Evidence suggests that zirconia- and hafnia-based coatings are stable in water vapor environments to temperatures as high as 1,650°C.[67,68] Zirconia and hafnia (HfO_2) are also the primary oxides formed when ZrB_2- or HfB_2-based UHTCs are oxidized. These materials are proposed for use at temperatures as high as 2,000°C for short-term exposures.[63] Based on Krikorian's estimated data for Y-O-H and Zr-O-H species,[69] it appears that yttria and zirconia are stable for long-term applications to temperatures as high as 1,902°C and >1,927°C, respectively, for a process at 0.1 MPa containing 10^{-2} MPa water vapor.[2] However, experimentally derived thermodynamic data for Y-O-H and Zr-O-H species are not available. These data would be very difficult to obtain because the temperatures for significant hydroxide formation are expected to be very high. At this time yttria, zirconia, and hafnia appear to be the most stable oxides in high-temperature water-vapor-containing environments.

Additional thermodynamic data are available for other gaseous metal-hydroxide and oxyhydroxide species. Not all the data have been confirmed as accurate, and in many cases no experimental data exist at all. A recent paper summarizes the known experimental data for metal-hydroxide and oxyhydroxide thermodynamic data.[70]

CONCLUSIONS

Most oxides form vapor-phase hydroxides or oxyhydroxides in high-temperature water vapor. Reliable thermodynamic data are available for $Si(OH)_4(g)$ and $Al(OH)_3(g)$, whereas the data for $CrO_2(OH)_2(g)$ vary widely. A recent study has tried to rectify this situation, but the results need confirmation. Accurate thermodynamic data for gaseous hydroxides are needed to calculate volatility of oxides in high-temperature water vapor and thus enable lifetime prediction for oxide materials in a variety of technologically important applications.

References

1. N.S. Jacobson, *NASA TP3162* (Washington, D.C.: NASA, 1992).
2. E.J. Opila and N.S. Jacobson, *Fundamental Aspects of High Temperature Corrosion*, ed. D.A. Shores, R.A. Rapp, and P.Y. Hou (Pennington, NJ: The Electrochemical Society, Inc., 1997), pp. 269–280.

3. G.R. Belton and F.D. Richardson, *Trans. Faraday Soc.,* 50 (1962), pp. 1562–1572.
4. E.J. Opila, *J. Am. Ceram. Soc.,* 82 (3) (1999), pp. 625–636.
5. E.J. Opila and D.L. Myers, *J. Am. Ceram. Soc.,* 87 (9) (2004), pp. 1701–1705.
6. Y.-W. Kim and G.R. Belton, *Met. Trans.,* 5 (1974), pp. 1811–1816.
7. D. Caplan and M. Cohen, *J. Electrochem. Soc.,* 108 (5) (1961), pp. 438–442.
8. C.S. Tedmon, Jr., *J. Electrochem. Soc.,* 113 (8) (1966), pp. 766–768.
9. E.J. Opila and R.E. Hann, *J. Am. Ceram. Soc.,* 80 (1) (1997), pp. 197–205.
10. E.J. Opila, *J. Am. Ceram. Soc.,* 86 (8) (2003), pp. 1238–1248.
11. J. Drowart and P. Goldfinger, *Angewandte Chemie,* 6 (7) (1967), pp. 581–596.
12. D.L. Hildenbrand and K.H. Lau, *J. Chem. Phys.,* 101 (7) (1994), pp. 6076–6079.
13. D.L. Hildenbrand and K.H. Lau, *J. Chem. Phys.,* 108 (15) (1998), p. 6535.
14. D.J. Meschi, W.A. Chupka, and J. Berkowitz, *J. Chem. Phys.,* 33 (2) (1960), pp. 530–533.
15. E. Opila, *Cer. Eng. & Sci. Proc.,* 26 (8) (2005), pp. 311–322.
16. C.A. Stearns et al., *NASA TM73720* (Washington, D.C.: NASA, 1977).
17. J.L. Margrave, *The Characterization of High Temperature Vapors* (New York: John Wiley & Sons, 1967).
18. U. Merten and W.E. Bell, *The Characterization of High Temperature Vapors*, ed. J.L. Margrave (New York: John Wiley & Sons, 1967), pp. 91–114.
19. A. Hashimoto, *Geochim. Cosmochim. Acta,* 56 (1992), pp. 511–532.
20. N.S. Jacobson et al., *J. Chem. Thermo.,* 37 (2005), pp. 1130–1137.
21. G.H. Geiger and D.R. Poirier, *Transport Phenomena in Metallurgy* (Reading, MA: Addison-Wesley Publishing Company, 1980), p. 532.
22. D.R. Gaskell, *An Introduction to Transport Phenomena in Materials Engineering* (New York: Macmillan Publishing Company, 1992), p. 573.
23. K.S. Pitzer and L. Brewer, *Thermodynamics*, 2nd ed. (New York: McGraw Hill Book Company, 1961), ch. 27.
24. C.F. Melius, M.D. Allendorf, and M.E. Colvin, *Proceedings of the 14th International Conference on CVD/EUROCVD11*, ed. M.D. Allendorf and C. Bernard (Pennington, NJ: The Electrochemical Society, Inc., 1997), pp. 1–14.
25. K. Hilpert et al., *J. Electrochem. Soc.,* 143 (1996), p. 3642.
26. J. Fergus, *Mat. Sci. Eng. A, 397*, 271, (2005).
27. H. Asteman et al., *Ox. Met.,* 52 (1999), p. 95.
28. A. Yamauchi, K. Kurokawa, and H. Takahashi, *Ox. Met.,* 59 (5/6) (2003), p. 517.
29. B.B. Ebbinghaus, *Combust. Flame,* 93 (1993), p. 119.
30. J. O'Leary, R. Kunz, and T. von Alten, *Environ. Prog.,* 23 (2004), p. 194.
31. J. Bailey, *J. Electrochem. Soc.,* 144 (1997), p. 3568.
32. H.C. Graham and H.H. Davis, *J. Am. Ceram. Soc.,* 54 (1971), p. 89.
33. G.C. Fryburg et al., *J. Electrochem. Soc.,* 124 (1977), p. 1738.
34. M. Farber and R.D. Srivastava, *Combust. Flame,* 20 (1973), p. 43.
35. C. Gindorf, L. Singheiser, and K. Hilpert, *J. Phys. Chem. Solids,* 66 (2005), p. 384.
36. C. Gindorf, K. Hilpert, and L. Singheiser, *Solid Oxide Fuel Cells VII*, ed. H. Yokokawa and S.C. Singhal (Pennington, NJ: The Electrochemical Society Inc., 2001), p. 793.
37. *IVTANTHERMO for Windows*, version 3.0, (1992–2003), w*ww.openweb.ru/thermo/index_eng.htm.*
38. Ø. Espelid, K.J. Børve, and V.R. Jense, *J. Phys. Chem. A,* 102 (1998), p. 10414.
39. E.J. Opila et al., submitted to *J. Phys. Chem. A.*
40. J.S. Smialek et al., *Adv. Comp. Mater.,* 8 (1) (1999), pp. 33–45.
41. H. Klemm, *J. Eur. Ceram. Soc.,* 22 (2002), pp. 2735–2740.
42. I. Yuri and T. Hisamatsu (Paper GT2002-38886 presented at the ASME Turbo Expo, 2003).
43. K.L. More et al. (Paper 99-GT-292 presented at the ASME Turbo Expo, 1999).
44. Z. Yao, J. Stiglich, and T.S. Sudarshan, *J. Mat. Eng. Perf.,* 8 (3) (1999), pp. 291–304.
45. J.J. Petrovic, *Cer. Eng. Sci. Proc.,* 18 (3) (1997), pp. 3–17.
46. A. Luttge et al., *Eur. J. Mineral.,* 10 (1998), pp. 385–389.
47. M.D. Allendorf et al., *J. Phys. Chem.,* 99 (1995), pp. 15285–15293.
48. E.J. Opila, D.S. Fox, and N.S. Jacobson, *J. Am. Ceram. Soc.,* 80 (4) (1997), pp. 1009–1012.
49. R.C. Robinson and J.L. Smialek, *J. Am. Ceram. Soc.,* 82 (7) (1999), pp. 1817–1825.
50. C.L. Darling and H.B. Schlegel, *J. Phys. Chem.,* 97 (1993), pp. 8207–8211.
51. M.W. Chase, Jr. et al., editors, *JANAF Thermochemical Tables*, 3rd ed. (New York: American Chemical Society and American Physical Society, 1985).
52. B.E. Deal and A.S. Grove, *J. Appl. Phys.,* 36 (12) (1965), pp. 3770–3778.
53. K.N. Lee, *Surf. Coating Tech.,* 133-134 (2000), pp. 1–7.
54. H.E. Eaton and G.D. Linsey, *J. Eur. Ceram. Soc.,* 22 (2002), pp. 2741–2747.
55. I. Spitzberg and J. Steibel, *Int. J. Appl. Ceram. Technol.,* 1 (4) (2004), pp. 291–301.
56. K.N. Lee et al., *J. Am. Ceram. Soc.,* 86 (8) (2003), pp. 1299–1306.
57. K.N. Lee, D.S. Fox, and N.P. Bansal, *J. Eur. Ceram. Soc.,* 25 (2005), pp. 1705–1715.
58. R.J. Kerans et al., *J. Am. Ceram. Soc.,* 85 (11) (2002), pp. 2599–2632.
59. R. Gadow and M. Lischka, *Surf. Coating Tech.,* 151-152 (2002), pp. 392–399.
60. M.D. Allendorf et al., *J. Phys. Chem. A,* 106 (2002), pp. 2629–2640.
61. N.S. Jacobson et al., *J. Am. Ceram. Soc.,* 82 (6) (1999), pp. 1473–1482.
62. R. Naslain et al., *J. Solid State Chem.,* 177 (2) (2004), pp. 449–456.
63. M.M. Opeka, I.G. Talmy, and J.A. Zaykoski, *J. Mat. Sci.,* 39 (2004), pp. 58878–58904.
64. R. Sakidja and J.H. Perepezko, *Metallurgical and Materials Transactions A: Physical Metallurgy and Materials Science,* 36A (3) (2005), pp. 507–514.
65. V. Behrani et al., *Intermetallics,* 14 (1) (2006), pp. 24–32.
66. N.S. Jacobson et al., *J. Am. Ceram. Soc.,* 82 (2) (1999), pp. 393–398.
67. D. Zhu, N.P. Bansal, and R.A. Miller, *NASA/TM-2003-212544* (Washington, D.C.: NASA, 2003).
68. D. Zhu et al., *NASA/TM-2004-213219* (Washington, D.C.: NASA, 2004).
69. O.H. Krikorian, *High Temp. High Pressures,* 14 (1982), pp. 387–397.
70. N. Jacobson et al., *J. Phys. Chem. Solids,* 66 (2005), pp. 471–478.

Elizabeth J. Opila, Nathan S. Jacobson, and Evan H. Copland are with NASA Glenn Research Center in Cleveland, Ohio. Copland is also with Case Western Reserve University in Cleveland, Ohio. Dwight L. Myers is with East Central University in Ada, Oklahoma.

For more information, contact Elizabeth J. Opila, NASA Glenn Research Center, MS 106-1, 21000 Brookpark Road, Cleveland, OH 44135; (216) 433-8904; fax (216) 433-5544; e-mail opila@grc.nasa.gov.